Strong Coupling Limit of the Holstein-Hubbard Model

Zhaoyu Han[®], ¹ Steven A. Kivelson[®], ^{1,*} and Hong Yao[®], ^{2,1,†} ¹Department of Physics, Stanford University, Stanford, California 94305, USA ²Institute of Advanced Study, Tsinghua University, Beijing 100084, China

(Received 9 July 2020; accepted 15 September 2020; published 13 October 2020)

We analyze the quantum phase diagram of the Holstein-Hubbard model using an asymptotically exact strong coupling expansion. We find all sorts of interesting phases including a pair-density wave, a charge 4e (and even a charge 6e) superconductor, regimes of phase separation, and a variety of distinct charge-density-wave, spin-density-wave, and superconducting regimes. We chart the crossovers that occur as a function of the degree of retardation, i.e., the ratio of characteristic phonon frequency to the strength of interactions.

DOI: 10.1103/PhysRevLett.125.167001

Typically, in strongly correlated materials, both direct electron-electron interactions and electron-phonon interactions are strong. Nonetheless, most theoretical studies focus exclusively on one or the other. The most widely studied model of the interplay between electron-electron (e-e) and electron-phonon (e-ph) interactions is the Holstein-Hubbard model [1–31]. The majority of existing studies are numerical explorations, despite the fact that the problem is complicated by the existence of multiple energy scales and a large parameter space. Monte Carlo studies of this problem are also generically rendered difficult by the fermion minus sign problem [32]. In this Letter, we systematically explore the "strong coupling" regimes in which the interactions are larger than the bandwidth, and a variety of results are derived from a theoretically wellcontrolled perturbative expansion. Qualitative results are summarized in the schematic phase diagram in Fig. 3.

The Holstein-Hubbard model is defined as

$$\begin{split} \hat{H} &= -t \sum_{\langle i,j \rangle, \sigma} (\hat{c}_{i,\sigma}^{\dagger} \hat{c}_{j,\sigma} + \text{H.c.}) - \mu \sum_{j} \hat{n}_{j} \\ &+ \frac{U_{e-e}}{2} \sum_{i} \hat{n}_{i}^{2} + \alpha \sum_{i} \hat{n}_{i} \hat{x}_{i} + \sum_{i} \left[\frac{\hat{p}_{i}^{2}}{2m} + \frac{k \hat{x}_{i}^{2}}{2} \right], \quad (1) \end{split}$$

where $\langle i,j \rangle$ signifies pairs of nearest-neighbor sites, $\hat{c}_{j\sigma}$ annihilates an electron with spin polarization σ on site $j, \hat{n}_j = \sum_{\sigma} \hat{c}^{\dagger}_{j\sigma} \hat{c}_{j\sigma}$ is the number operator on site j, x_j is an optical phonon coordinate at site j, and p_j is the conjugate momentum. The dominant effects of strong electron-phonon coupling can be accounted for by a unitary transformation $\hat{U} \equiv \prod_i \exp\left[i(\alpha/k)\,\hat{p}_i\hat{n}_i\right]$ [33]. The transformed Hamiltonian is

$$\hat{U}^{\dagger} \hat{H} \, \hat{U} = -t \sum_{\langle i,j \rangle, \sigma} (\hat{S}_{ij} \hat{c}_{i,\sigma}^{\dagger} \hat{c}_{j,\sigma} + \text{H.c.}) - \mu \sum_{j} \hat{n}_{j}$$

$$+ \frac{U_{\text{eff}}}{2} \sum_{i} \hat{n}_{i}^{2} + \sum_{i} \left[\frac{\hat{p}_{i}^{2}}{2m} + \frac{k \hat{x}_{i}^{2}}{2} \right], \qquad (2)$$

where $\hat{S}_{ij} \equiv \exp\left[i(\alpha/k)(\hat{p}_j - \hat{p}_i)\right]$ is a product of two phonon displacement operators on site i and j, $U_{\rm eff} \equiv U_{e-e} - U_{e-\rm ph}$, and $U_{e-\rm ph} \equiv \alpha^2/k$. This transformation is exact and can be alternatively derived by a path integral representation tracking the phonon degrees of freedom in momentum space [34].

In the strong coupling expansion, we treat the hopping term in the transformed Hamiltonian as a perturbation, and the sign of $U_{\rm eff}$ determines the relevant low-energy degrees of freedom. The resulting theories are generic regardless of lattice structure and dimensionality, but to have explicit examples in mind, we will mainly consider the 2D square and triangular lattices. We focus on the behavior of the model at temperature T=0, although we also make estimates of the parametric dependence of the critical temperatures [39]. Without loss of generality, we will consider the case in which the average number of electrons per site $n \equiv N^{-1} \sum_{i=1}^{N} \langle \hat{n}_{i} \rangle \leq 1$, and will refer to x = 1 - nas the "concentration of doped holes." (A particle-hole transformation $\hat{c} \leftrightarrow \hat{c}^{\dagger}$ relates this problem to an electrondoped problem with n = 1 + x and with opposite sign of hopping t and e-ph coupling α .) Explicit calculations are deferred to the Supplemental Material [34].

 $For \, U_{\rm eff} > 0$.—The ground-state manifold to zeroth order in t consists of all states with no doubly occupied sites and no phonons. Performing degenerate perturbation theory up to second order yields an effective Hamiltonian (leaving implicit projection onto the space of no doubly occupied sites and Hermitian conjugation of quantum hopping terms):

$$\hat{H}_{\text{eff}} = -t_1 \sum_{\langle i,j \rangle, \sigma} \hat{c}_{i,\sigma}^{\dagger} \hat{c}_{j,\sigma} - t_2 \sum_{\langle i,m,j \rangle, \sigma} \hat{c}_{i,\sigma}^{\dagger} (1 - 2\hat{n}_m) \hat{c}_{j,\sigma}$$

$$- (\tau + 2t_2) \sum_{\langle i,m,j \rangle} \hat{s}_{im}^{\dagger} \hat{s}_{mj} + J \sum_{\langle i,j \rangle} \left[\vec{S}_i \cdot \vec{S}_j - \frac{\hat{n}_i \hat{n}_j}{4} \right]$$

$$+ V \sum_{\langle i,j \rangle} \hat{n}_i \hat{n}_j, \tag{3}$$

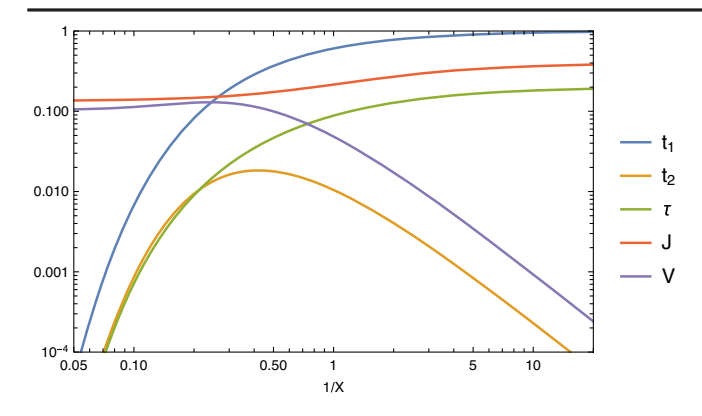


FIG. 1. An illustration of the coefficients as functions of the degree of retardation $1/X=(\omega_D/U_{e\text{-ph}})$, with fixed $U_{e\text{-e}}=30$, $U_{e\text{-ph}}=20$, and t=1.

where t_1 is the (renormalized) nearest-neighbor hopping, t_2 is a next-nearest-neighbor hopping term via an intermediate site m, and $\langle i, m, j \rangle$ represents a triplet of sites such that m is a nearest neighbor of two distinct sites i and j, $(\tau + 2t_2)$ is a singlet hopping term where $\hat{s}_{ij} = (\hat{c}_{i,\uparrow}\hat{c}_{j,\downarrow} + \hat{c}_{j,\uparrow}\hat{c}_{i,\downarrow})/\sqrt{2}$ is the annihilation operator of a singlet Cooper pair on bond $\langle ij \rangle$, J is the antiferromagnetic exchange interaction, and V is the repulsion between electrons on nearest-neighbor sites.

The values of these effective couplings can be computed explicitly in terms of the dimensionless functions,

$$F(x,y) \equiv ye^{-|x|} \int_0^\infty dt e^{-yt + xe^{-t}},$$
 (4)

$$F'(x) \equiv x \frac{\partial F}{\partial y}\Big|_{y \to 0} = xe^{-|x|} \int_0^\infty dt (e^{xe^{-t}} - 1) \qquad (5)$$

of the dimensionless parameters $X \equiv U_{e\text{-ph}}/\omega_D$ and $Y \equiv |U_{\text{eff}}|/\omega_D$ as shown in the first column of Table I, where $\omega_D = \sqrt{k/m}$ is the optical phonon frequency. Explicit asymptotic expressions for these functions can be obtained in the large and small ω_D limit, as listed in the second and third columns of the table. In Fig. 1, we show the coefficients in Eq. (3), as functions of X for given values of $U_{e\text{-}e}$, $U_{e\text{-}ph}$, and t. Increasing the e-ph coupling or lowering the phonon frequency suppresses quantum hopping and thus any tendency toward superconductivity.

This suppression is a manifestation of the self-trapping crossover of the single polaron problem. Increasing the *e*-ph coupling also enhances the spin fluctuations, which is consistent with a previous study [17].

In the antiadiabatic limit $\omega_D \to \infty$, the *e-e* and *e-*ph interactions are simply additive, so the effective theory is identical to the standard *t-J* model generated by a Hubbard model with $U = U_{\rm eff} > 0$. In this limit, $|t_1| \gg J$ and V as usually considered. This hierarchy remains valid in a range of smaller ω_D . While this limit is interesting and has been widely studied, there is no qualitatively new physics associated with the presence of phonons.

As the phonon frequency is lowered, J and V approach constants, but quantum hoppings are rapidly suppressed, reflecting the effect of a Frank-Condon overlap factor [40]. In the adiabatic limit $\omega_D \to 0$, the effective model is realized in the limit $|t_1| \ll J$, V, which was previously considered to be unphysical. The effective model is now similar to the small t limit of the t-J-V model studied in Ref. [41], with the difference that there can also be other smaller hopping terms, t_2 and τ . A schematic diagram of possible phases that arise in this limit on the triangular lattice can be seen in Fig. 2(a); a similar phase diagram was discussed for the square lattice in Fig. 3 of Ref. [41]. The nature of the resulting phases can be seen by neglecting the hopping terms to zeroth order.

Insulating charge- and spin-density-wave phases.— $V/J \ll 1$ leads to two-phase phase coexistence of an insulating antiferromagnet with x=0 and an electron-free void with x=1, i.e., complete phase separation of the doped holes. At larger values of V/J, the phase diagram is more complicated. Generally, for most values of x smaller than a critical value x_c (which depends on both the lattice geometry and the value of V/J), the doped holes form various forms of commensurate hole crystals coexisting with some form of antiferromagnetic order, likely forming some form of two-phase coexistence between two such phases. An example of this is the $\sqrt{5} \times \sqrt{5}$ hole crystal with x=1/5 discussed for the square lattice in Ref. [41], and an analogous $\sqrt{7} \times \sqrt{7}$ hole crystal that likely arises on the triangular lattice with x=1/7.

A variety of more unusual behaviors arise at lower electron density. When $x > x_c$, the system can be thought

TABLE I. The expressions and the limiting behaviors of the coefficients in the effective theory in Eq. (3).

	$\omega_D \to 0$	$\omega_D o \infty$
	$(X,Y\to\infty)$	$(X, Y \to 0)$
$t_1 = te^{-X/2}$	$te^{-X/2}$	t
$t_2 = (2t^2/U_{e-\text{ph}})e^{-X/2}F'(X/2)$	$(2t^2/U_{e\text{-ph}})e^{-X/2}$	$t^2 X^2 / 2U_{e\text{-ph}}$
$\tau = (2t^2/U_{\text{eff}})e^{-X/2}F(X/2, Y)$	$4t^2/(U_{\rm eff}+U_{e-e})e^{-X/2}$	$2t^2/U_{\mathrm{eff}}$
$J = (4t^2/U_{\rm eff})F(X,Y)$	$4t^2/U_{e-e}$	$4t^2/U_{\mathrm{eff}}$
$V = (2t^2/U_{e\text{-ph}})F'(X)$	$(2t^2/U_{e ext{-ph}})$	$(2t^2X^2/U_{e\text{-ph}})$

of as a dilute collection of electrons, which form small disconnected clusters. The effect of the relatively smaller hopping terms then resolves remaining ground-state degeneracy by degenerate perturbation theory.

Heavy Fermi liquid.—For large V/J > 1, monomers are favored to the zeroth order. Extensively degenerate ground states consist of all configurations where no pair of nearest-neighbor sites is occupied. When the hopping terms are included, these monomers can be treated as spin-1/2 fermions with a hard-core radius that extends to nearest-neighbor sites and a highly renormalized hopping matrix element t_1 . Typically, we would expect this system to form a heavy Fermi liquid, although at various commensurate values of x, via "order by disorder," it may well exhibit commensurate charge-density-wave (CDW) order with some form of accompanying spin-density-wave (SDW) order [42]. It also can have a very low T Kohn-Luttinger-type instability to unconventional superconductivity [43].

Hard-core dimer fluid.—For $\nu_2 < V/J < 1$ (where $\nu_2 = 0.5$ and 0.43 for the square and triangular lattices, respectively), singlet pairs of electrons on nearest-neighbor bonds are energetically optimal. These dimers are elliptical hard-core bosons [44], and the zeroth order ground states can be labeled by dimer configurations where the dimers satisfy both a hard-core constraint (no two dimers touch the same site) and a nearest-neighbor exclusion (no pair of nearest-neighbor sites is touched by distinct dimers).

The ground-state degeneracy is lifted when the effect of hopping terms is included. While at special commensurate densities, this could lead to an insulating CDW phase, generically it leads to charge 2e singlet superfluid phases of various sorts. To address the nature of these phases, we write the effective model of hard-core dimers,

$$\hat{H}_{\text{dimer}} = -\sum_{\langle ij\rangle,\langle mn\rangle} (\tau_{ij,mn} \hat{s}_{ij}^{\dagger} \hat{s}_{mn} + \text{H.c.}), \tag{6}$$

where $\tau_{ij,mn}$ is the effective pair hopping amplitude between bond $\langle ij \rangle$ and bond $\langle mn \rangle$. There are various

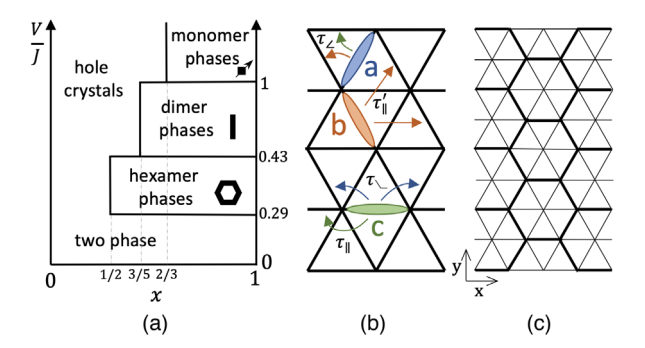


FIG. 2. For the triangular lattice, (a) a schematic phase diagram for the $t_1 \ll J$, V model, (b) an illustration of various pair-hopping terms appearing in \hat{H}_{dimer} [Eq. (6)], and (c) a possible PDW pattern, the thickened bonds have pair field proportional to $+\phi$ and others $-\phi/2$, where ϕ is the amplitude.

distinct types of hopping processes that can arise up to second order in t and contribute to different sorts of dimer hopping amplitudes. Generically, dimers can be moved by the singlet-pair hopping $(\tau + 2t_2)$ and next-nearest-neighbor hopping t_2 . (Another virtual process with amplitude $(t_1^2/J - V)$ can also hop dimers, but it is unimportant in the adiabatic limit since it is suppressed relative to the terms we have kept by a factor of $e^{-X/2}$.) These processes in the second order of t all make positive contributions to $\tau_{ij,mn}$, independent of the sign of t. When all $\tau_{ij,mn} \geq 0$, the $-\hat{H}_{\text{dimer}}$ satisfies the conditions of Perron-Frobenius theorem [45], and hence, the Hamiltonian is minimized by a Bloch state with $\vec{k} = \vec{0}$ and all positive amplitudes. Since at finite dimer density, the system likely forms a Bose condensate, this implies the pair field is spatially uniform on square and most lattices.

However, on the triangular lattice (or other frustrated geometries), dimers can hop via a first order process in t_1 . This process contributes to the type of pair hopping labeled τ_{\perp} in Fig. 2(b), in which one end of a dimer pivots by 60° about the other end, and it has much larger amplitude than auand t_2 . Consequently, τ_{\angle} has the same sign as t, and is larger in magnitude than the remaining terms $\tau_{\parallel},~\tau_{\parallel}',$ and τ . This opens the possibility of exotic condensation when t < 0. On a triangular lattice, there are three possible dimer states per unit cell, and correspondingly, three bands. Taking into account only the largest pair-hopping term $\tau_{/}$, these consist of a flat band and two dispersing bands, such that the flat band is the lowest if t < 0. Including the effects of the smaller pair-hopping terms, we find the band minima occur at the K and -K points in the Brillouin zone. A dimer Bose condensate thus results in some form of a PDW [46]. A state in which the condensed bosons have momentum either K or -K breaks time-reversal symmetry but has a spatially uniform magnitude of pair field. If timereversal symmetry is preserved, singlets equally condense in $\pm K$, resulting in a translation symmetry breaking pattern of the pair field, as shown in Fig. 2(c). Which form of condensate is favored remains to be determined due to the strongly interacting nature of bosons in the present problem, although it was shown that the plane-wave state is favored for the case of weakly interacting bosons [47]. For a Bose condensate at either the Γ or K point, the curvature of the band bottom is set by terms to the second order in t, and the superconducting transition temperature is parametrically small $T_c \sim t^2 e^{-X/2}$ in the adiabatic limit.

Polygonal fluid.—Further reducing V/J, different lattices lead to different optimal clusters. On a square lattice, a tetramer (square) minimizes the energy for $\nu_4 < V/J < \nu_2 = 0.5$, and phase separation occurs for $V/J < \nu_4 = 0.418$. On a triangular, honeycomb, or kagome lattice, a hexamer minimizes the energy for $\nu_6 < V/J < \nu_2 = 0.434$, and phase separation occurs for $V/J < \nu_6 = 0.290$ (triangle), 0.390 (honeycomb), 0.215 (Kagome).

TABLE II. The expressions and the limiting behaviors of the coefficients in the effective theory in Eq. (7).

	$\omega_D o 0$	$\omega_D o \infty$
$t_b = (2t^2/ U_{\text{eff}})F(-X,Y)$	$(2t^2/ U_{\rm eff})(U_{e{\rm -ph}}/U_{e{\rm -e}})e^{-(X+Y)}$	$(2t^2/ U_{\rm eff})$
$V_b = (4t^2/ U_{\text{eff}})F(X,Y)$	$4t^2/(U_{e ext{-ph}} + U_{ ext{eff}})$	$4t^2/ U_{\mathrm{eff}} $

These clusters are hard-core bosons with nearest-neighbor exclusion that can condense into charge 4e or 6e superconducting phases. The quantum hopping of these clusters derives from a high order process, so the superconducting transition temperature should be low and upper bounded by t_1^p , where p is the number of electrons in the cluster.

It is not always the case that the simple Holstein-Hubbard model can realize all the interesting ranges of V/J. In particular, in the adiabatic limit, $V/J = (U_{e-e}/2U_{e-ph}) > 0.5$. However, the introduction of weak dispersion of the phonons or longer-ranged coupling to the electron densities will introduce nearest-neighbor attraction in the zeroth order that can be easily comparable with J and drive the system into the interesting cluster phases. As a concrete example, adding weak phonon coupling to nearest-neighbor sites $\hat{H}' = \sum_{\langle i,j \rangle} \alpha'(\hat{n}_i + \hat{n}_j)(\hat{x}_i + \hat{x}_j)$ introduces a small nearest-neighbor attraction α'^2/k without modifying the hopping terms.

For $U_{\rm eff} < 0$.—The degenerate ground-state manifold in the absence of hopping consists of states occupied by pairs of electrons (on-site bipolarons) and no phonon. Including hopping in degenerate perturbation theory yields

$$\hat{H}_{\text{eff}} = -t_b \sum_{\langle i,j \rangle} (\hat{b}_i^{\dagger} \hat{b}_j + \text{H.c.}) + V_b \sum_{\langle i,j \rangle} \hat{b}_i^{\dagger} \hat{b}_i \hat{b}_j^{\dagger} \hat{b}_j, \quad (7)$$

where $\hat{b}_i \equiv \hat{c}_{i,\uparrow} \hat{c}_{i,\downarrow}$ annihilates a hard-core boson on site i $(\hat{b}_i^{\dagger}\hat{b}_i = 0, 1 \text{ is implicitly imposed}).$ t_b and V_b are, respectively, the nearest-neighbor hopping and repulsion whose values are listed in Table II. This is a standard hardcore boson model (or equivalently, a spin-1/2 XXZ model), for which superfluidity and charge orders were investigated on various lattices [48-52]. Below a Kosterlitz-Thouless transition $\sim t_b$, superfluidity is possible. This transition temperature is also parametrically small, $T_c \lesssim (t^2/t^2)$ $|U_{\rm eff}|)e^{-X}$. Particular interesting possibilities are supersolid phases on frustrated lattices, where the predicted phase region $t_b \le 0.1 V_b$ for the triangular lattice [51] is clearly accessible through tuning retardation. Indeed, coexisting superconducting and charge orders were predicted theoretically [8] and have been seen in a recent study of the triangular lattice Holstein model [53]. Above the superfluid transition temperature, but below the binding energy $|U_{\rm eff}|$, the system is essentially a classical bipolaron gas, where various commensurate charge orders and phase separations can exist below an Ising critical temperature $\sim V_h$ [27]. Increasing the e-e repulsion can enhance charge and especially superconducting order, in contrast to a previous study on the weak coupling regime [6].

Range of validity of the effective theories.—The effective models we have derived operate in reduced Hilbert spaces with restricted site occupancies (determined by the sign of $U_{\rm eff}$) and zero phonon excitations. These restrictions become invalid when excitation energies in the unperturbed Hamiltonian are no longer large compared with the corresponding perturbation matrix elements. Specifically, all possible site occupancies should be considered when $|U_{\rm eff}| \lesssim |t_1| = |t|e^{-X/2}$, and phonon excitations should be included if $\omega_D \lesssim |t_1| \sqrt{X/2}$. These narrow regions are enclosed with solid lines and hashed out in the schematic phase diagram in Fig. 3.

Within the reduced Hilbert space, there remains the issue of whether it is sufficient to compute the effective interactions to low order in powers of |t|. This is controlled so long as the longer-ranged interactions generated by higher order terms are small compared with the terms we have already considered. This sort of analysis was carried out for the strong coupling limit of Holstein and Hubbard models in Refs. [2,54]. For the mth order of the $J^{(m)}$, $V^{(m)}$, or $V^{(m)}_b$ series, we have evaluated the amplitudes of virtual processes involving hopping around m sites and regard them as

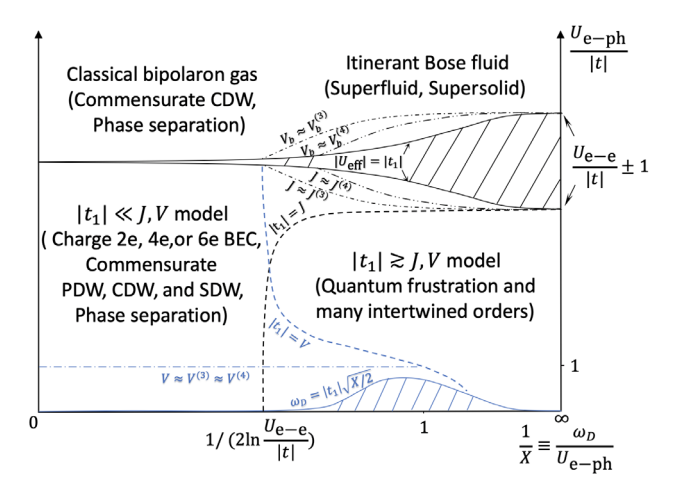


FIG. 3. A schematic phase diagram of the Holstein-Hubbard model in the strong coupling limit. The black or blue dashed lines separate large and small $|t_1|/J$ or $|t_1|/V$ regimes. The meanings of the other lines are discussed in the text and correspond to the indicated equalities. The condition $V = V^{(m)}$ is not plotted to region $V < |t_1|$, since all orders of $V^{(m)}$ are small compared to quantum hopping in this region.

representative. The condition (valid so long as $U_{e\text{-}e}\gg |U_{\text{eff}}|\sim |t|)$ for $J\gg J^{(m)}$ and $V_b\gg V_b^{(m)}$ is $|U_{\text{eff}}|\gg \min\{|t|,r_mU_{e\text{-ph}}e^{-X}\},$ where $r_m\equiv [m/2(m-1)].$ Similarly, $V\gg V^{(m)}$ so long as $U_{e\text{-ph}}\gg |t|\min\{1,X\,2^{-1/(m-2)}\}.$ The black and blue dashed-dotted lines in Fig. 3 are thus defined, as indicated by the estimation $J\approx J^{(m)},\ V_b\approx V_b^{(m)},$ or $V\approx V^{(m)}$ for m=3 (for the triangular lattice) and m=4 (for the square lattice). Longer-ranged interactions are significant inside these lines.

S. A. K. was supported, in part, by NSF Grant No. DMR-2000987 at Stanford. H. Y. was supported in part by National Science Fund for Distinguished Young Scholars of NSFC through Grant No. 11825404 at Tsinghua, by the Technology Ministry of Science and China under Grants No. 2016YFA0301001 and No. 2018YFA0305604 and by the Gordon and Betty Foundations **EPiQS** Moore through Grant No. GBMF4302 at Stanford.

- *kivelson@stanford.edu
 †yaohong@tsinghua.edu.cn
- [1] J. Zhong and H.-B. Schüttler, Phys. Rev. Lett. **69**, 1600 (1992).
- [2] J. K. Freericks, Phys. Rev. B 48, 3881 (1993).
- [3] J. K. Freericks and M. Jarrell, Phys. Rev. B 50, 6939 (1994).
- [4] H. Fehske, D. Ihle, J. Loos, U. Trapper, and H. Büttner, Z. Phys. B 94, 91 (1994).
- [5] E. Berger, P. Valášek, and W. von der Linden, Phys. Rev. B 52, 4806 (1995).
- [6] J. K. Freericks and M. Jarrell, Phys. Rev. Lett. 75, 2570 (1995).
- [7] G. Wellein, H. Röder, and H. Fehske, Phys. Rev. B 53, 9666 (1996).
- [8] J. Stein, Europhys. Lett. 39, 413 (1997).
- [9] L. Proville and S. Aubry, Physica (Amsterdam) 113D, 307 (1998).
- [10] J. Bonča and S. A. Trugman, Phys. Rev. B 64, 094507 (2001).
- [11] Y. Takada and A. Chatterjee, Phys. Rev. B **67**, 081102(R) (2003).
- [12] M. Capone, G. Sangiovanni, C. Castellani, C. Di Castro, and M. Grilli, Phys. Rev. Lett. 92, 106401 (2004).
- [13] A. Macridin, G. A. Sawatzky, and M. Jarrell, Phys. Rev. B 69, 245111 (2004).
- [14] W. Koller, D. Meyer, and A. C. Hewson, Phys. Rev. B 70, 155103 (2004).
- [15] W. Koller, D. Meyer, Y. Ōno, and A. C. Hewson, Europhys. Lett. **66**, 559 (2004).
- [16] E. W. Carlson, S. A. Kivelson, D. Orgad, and V. J. Emery, in The Physics of Superconductors: Vol. II. Superconductivity in Nanostructures, High-Tc and Novel Superconductors, Organic Superconductors, edited by K. H. Bennemann and J. B. Ketterson (Springer, Berlin, 2004), pp. 275–451.

- [17] A. Macridin, B. Moritz, M. Jarrell, and T. Maier, Phys. Rev. Lett. 97, 056402 (2006).
- [18] P. Werner and A. J. Millis, Phys. Rev. Lett. 99, 146404 (2007).
- [19] R. P. Hardikar and R. T. Clay, Phys. Rev. B **75**, 245103 (2007).
- [20] O. Gunnarsson and O. Rsch, J. Phys. Condens. Matter 20, 043201 (2008).
- [21] S. Kumar and J. van den Brink, Phys. Rev. B **78**, 155123
- [22] M. Hohenadler and F. F. Assaad, Phys. Rev. B 87, 075149 (2013).
- [23] S. Johnston, E. A. Nowadnick, Y. F. Kung, B. Moritz, R. T. Scalettar, and T. P. Devereaux, Phys. Rev. B 87, 235133 (2013).
- [24] P. Werner and M. Eckstein, Phys. Rev. B 88, 165108 (2013).
- [25] T. Ohgoe and M. Imada, Phys. Rev. Lett. 119, 197001 (2017).
- [26] S. Karakuzu, L. F. Tocchio, S. Sorella, and F. Becca, Phys. Rev. B 96, 205145 (2017).
- [27] M. Weber and M. Hohenadler, Phys. Rev. B **98**, 085405 (2018).
- [28] M. Hohenadler and H. Fehske, Eur. Phys. J. B 91, 204 (2018).
- [29] S. Karakuzu, K. Seki, and S. Sorella, Phys. Rev. B 98, 201108(R) (2018).
- [30] Y. Wang, I. Esterlis, T. Shi, J. I. Cirac, and E. Demler, arXiv:1910.01792.
- [31] S. Kazuhiro, Y. Seiji, S. Sandro *et al.*, Commun. Phys. 3, 80 (2020).
- [32] Z.-X. Li and H. Yao, Annu. Rev. Condens. Matter Phys. 10, 337 (2019).
- [33] M. Hohenadler and W. von der Linden, in *Polarons in Advanced Materials*, edited by A. S. Alexandrov (Springer, Dordrecht, 2007), pp. 463–502.
- [34] See Supplemental Material at http://link.aps.org/supplemental/10.1103/PhysRevLett.125.167001 and Refs. [35–38] therein for detailed discussions of the generalized Holstein-Lang-Firsov transformation, the calculation of various coefficients, and singlet pairing on the triangular lattice.
- [35] M. J. de Oliveira, Phys. Rev. B 48, 6141 (1993).
- [36] L. Capriotti, A. E. Trumper, and S. Sorella, Phys. Rev. Lett. 82, 3899 (1999).
- [37] J. D. Reger, J. A. Riera, and A. P. Young, J. Phys. Condens. Matter 1, 1855 (1989).
- [38] G. Evenbly and G. Vidal, Phys. Rev. Lett. 104, 187203 (2010).
- [39] To extend the effective theories to nonzero temperature T, we need to estimate the T scale above which their T dependence is significant. This is especially interesting when ω_D is small compared to t. To make this estimation, we perform perturbation theory averaged on the thermal equilibrium state of the phonons. We find that the values of the coefficients do not significantly change if $U_{e\text{-ph}}$, $|U_{\text{eff}}| \gg \omega_D \epsilon_\beta$ or $U_{e\text{-ph}}$, $|U_{\text{eff}}| \ll \omega_D/\epsilon_\beta$, where $\epsilon_\beta \equiv [(2e^{-\beta\omega_D})/(1-e^{-\beta\omega_D})]$. This is always satisfied for $T \ll \omega_D$.
- [40] M. Lax, J. Chem. Phys. 20, 1752 (1952).
- [41] S. A. Kivelson, V. J. Emery, and H. Q. Lin, Phys. Rev. B 42, 6523 (1990).

- [42] A. G. Green, G. Conduit, and F. Krger, Annu. Rev. Condens. Matter Phys. 9, 59 (2018).
- [43] W. Kohn and J. M. Luttinger, Phys. Rev. Lett. 15, 524 (1965).
- [44] In the context of bipolaron problem, extended versions of this have been called S1 bipolarons [9,13].
- [45] C. R. MacCluer, SIAM Rev. 42, 487 (2000).
- [46] D. F. Agterberg, J. S. Davis, S. D. Edkins, E. Fradkin, D. J. Van Harlingen, S. A. Kivelson, P. A. Lee, L. Radzihovsky, J. M. Tranquada, and Y. Wang, Annu. Rev. Condens. Matter Phys. 11, 231 (2020).
- [47] Y.-Z. You, Z. Chen, X.-Q. Sun, and H. Zhai, Phys. Rev. Lett. 109, 265302 (2012).

- [48] G. Schmid, S. Todo, M. Troyer, and A. Dorneich, Phys. Rev. Lett. 88, 167208 (2002).
- [49] Y.-C. Chen, R. G. Melko, S. Wessel, and Y.-J. Kao, Phys. Rev. B 77, 014524 (2008).
- [50] R. G. Melko, A. Paramekanti, A. A. Burkov, A. Vishwanath, D. N. Sheng, and L. Balents, Phys. Rev. Lett. 95, 127207 (2005).
- [51] F. Wang, F. Pollmann, and A. Vishwanath, Phys. Rev. Lett. 102, 017203 (2009).
- [52] S. Wessel, Phys. Rev. B 75, 174301 (2007).
- [53] Z.-X. Li, M. L. Cohen, and D.-H. Lee, Phys. Rev. B 100, 245105 (2019).
- [54] A. H. MacDonald, S. M. Girvin, and D. Yoshioka, Phys. Rev. B 37, 9753 (1988).